Atten Percept Psychophys (2014) 76:473–488
DOI 10.3758/s13414-013-0567-1

Perceptual adaptation to structure-from-motion depends on the size of adaptor and probe objects, but not on the similarity of their shapes

Alexander Pastukhov · Anna Lissner · Jochen Braun

Published online: 1 November 2013

Abstract Perceptual adaptation destabilizes the phenomenal appearance of multistable visual displays. Prolonged dominance of a perceptual state fatigues the associated neural population, lowering the likelihood of renewed perception of the same appearance (Nawrot & Blake in *Perception & Psychophysics*, *49*, 230–44, 1991). Here, we used a selective adaptation paradigm to investigate perceptual adaptation for the illusory rotation of ambiguous structure-from-motion (SFM) displays. Specifically, we generated SFM objects with different three-dimensional shapes and presented them in random order, separating successive objects by brief blank periods, which included a mask. To assess the specificity of perceptual adaptation to the shape of SFM objects, we established the probability that a perceived direction of rotation persisted between successive objects of similar or dissimilar shape. We found that the strength of negative aftereffects depended on the volume, but not the shape, of adaptor and probe objects. More voluminous objects were both more effective as adaptor objects and more sensitive as probe objects. Surprisingly, we found these volume effects to be completely independent, since any relationship between two shapes (such as overlap between volumes, similarity of shape, or similarity of velocity profiles) failed to modulate the negative aftereffect. This pattern of results was the opposite of that observed for *sensory memory* of SFM objects, which reflects similarity between objects, but not volume of individual objects (Pastukhov et al. in *Attention, Perception & Psychophysics*, *75*, 1215–1229, 2013). The disparate specificities of perceptual adaptation and sensory memory for identical SFM objects suggest that the two aftereffects engage distinct neural representations, consistent with recent brain imaging results (Schwiedrzik et al. in *Cerebral Cortex,* 2012).

Keywords 3D perception · Depth and shape from X · Binocular vision · Rivalry/Bistable perception · Perceptual implicit memory

Introduction

Our perception reflects both current sensory information and recent sensory experience. Over shorter periods (≤0.5 s), recent perception of a particular appearance can suppress the renewed perception of this appearance both in unambiguous and in ambiguous visual displays (Clifford et al., 2007; Nawrot & Blake, 1991; Pastukhov & Braun, 2011, 2013a, 2013b; Petersik, 2002; Webster, 2011; Wolfe, 1984). Over longer periods (>1 s), recent experience of a particular object appearance can also facilitate its renewed perception, again in both unambiguous and ambiguous visual displays. This has been reported in the context of repetition priming (Kristjánsson & Campana, 2010; Schacter, Wig, & Stevens, 2007), perceptual visual memory (Y. Tanaka & Sagi, 1998), and sensory memory of ambiguous perception (Adams, 1954; Daelli, van Rijsbergen, & Treves, 2010; Kornmeier, Ehm, Bigalke, & Bach, 2007; Leopold, Wilke, Maier, & Logothetis, 2002; Orbach, Ehrlich, & Heath, 1963; Pastukhov & Braun, 2008; Pearson & Brascamp, 2008). We will refer to these negative and positive history effects as *perceptual adaptation* and *sensory memory* (Pearson & Brascamp, 2008), respectively. We opted to use the term *perceptual adaptation*—rather than *visual adaptation*

Electronic supplementary material The online version of this article (doi:10.3758/s13414-013-0567-1) contains supplementary material, which is available to authorized users.

A. Pastukhov · A. Lissner · J. Braun
Center for Behavioral Brain Sciences, Magdeburg, Germany

A. Pastukhov (✉) · A. Lissner · J. Braun
Cognitive Biology, Otto-von-Guericke Universität, Magdeburg, Germany
e-mail: pastukhov.alexander@gmail.com

(Clifford et al., 2007) or *habituation* (Noest, van Ee, Nijs, & van Wezel, 2007)—to highlight that the aftereffect is specific to one particular perceptual state, not to an ambiguous display as a whole.

At the neural level, negative and positive priming effects are evident in the form of repetition suppression (Desimone, 1996; Grill-Spector, Henson, & Martin, 2006; Grill-Spector et al., 1999; Huk & Heeger, 2002) and/or repetition enhancement (Segaert, Weber, de Lange, Petersson, & Hagoort, 2013). These neural priming effects can be utilized to probe the feature specificity of neural representations (Schacter et al., 2007). For example, selective adaptation has been used to characterize neural selectivity for spatial frequency and orientation (Blakemore & Campbell, 1969), three-dimensional shape (Preston, Kourtzi, & Welchman, 2009), face identity (Leopold, O'Toole, Vetter, & Blanz, 2001), and other object features (Malach, 2012). Similarly, selective priming has helped to characterize the neural representation underlying structure-from-motion displays (Chen & He, 2004; Kristjánsson & Campana, 2010; Maier, Wilke, Logothetis, & Leopold, 2003; Pastukhov, Füllekrug, & Braun, 2013), the streaming-bouncing paradigm (Caplovitz, Shapiro, & Stroud, 2011; Feldman & Tremoulet, 2006; Kawachi, Kawabe, & Gyoba, 2011), and the Ternus display (Kramer & Rudd, 1999; Shechter, Hochstein, & Hillman, 1988; Yu, 2000).

The primary purpose of the present study was to investigate perceptual adaptation in structure-from-motion (SFM) displays: planar motion flows assuming the appearance of objects rotating in depth (Sperling & Dosher, 1994; Wallach & O'Connell, 1953) (please see Supplementary Movies). An earlier study by Nawrot and Blake (1991) demonstrated negative aftereffects with various SFM objects (sphere, cube, wire figure, two parallel planes) as adaptor and probe objects. Aftereffects seemed to depend neither on object identity nor on object similarity, since all adaptor–probe pairs produced robust aftereffects. We wished to reexamine the issue with a larger and more diverse set of SFM shapes. Recently, we demonstrated shape selectivity of sensory memory for SFM shapes (Pastukhov et al., 2013), revising the conclusions of an earlier study (Maier et al., 2003). This prompted us to take a similarly close look at perceptual adaptation to SFM shapes.

A secondary purpose was to compare and contrast the respective neural representations engaged by perceptual adaptation and sensory memory. Both priming effects engage motion-selective areas of the visual cortex (Brascamp, Kanai, Walsh, & van Ee, 2010; de Jong, Kourtzi, & van Ee, 2012; Fang, Murray, & He, 2007; Ganel et al., 2006; Smith & Wall, 2008; Sterzer & Rees, 2008; Walther, Schweinberger, Kaiser, & Kovács, 2012) and have been modeled in terms of a single fatigue variable (Brascamp, Knapen, Kanai, van Ee, & van den Berg, 2007; Brascamp, Pearson, Blake, & van den Berg, 2009; Gepshtein & Kubovy, 2005; Noest et al., 2007; Noest & van Wezel, 2012). The two priming effects are not identical, however, since sensory memory has a stronger impact on onset perception and perceptual adaptation on dominance durations (de Jong, Knapen, & van Ee, 2012). Also, sensory memory engages a network of fronto-parietal areas associated with attention and visual memory (de Jong, Kourtzi, & van Ee, 2012; Schwiedrzik et al., 2012; Sterzer & Rees, 2008), which suggests that it may involve distinct evidence and memory representations (Gigante, Mattia, Braun, & Del Giudice, 2009). By characterizing the respective shape selectivity of these two priming effects, we hoped to clarify the extent to which they involve overlapping neural representations.

To achieve these objectives, we used a variety of SFM objects differing in shape and solidity (hollow or filled) to establish the strength of perceptual adaptation between different object pairs. Identical sets of SFM objects were used in our companion study of sensory memory (Pastukhov et al., 2013). To facilitate comparison with earlier studies, we used both paired presentations (unambiguous adaptor followed by ambiguous probe, as in Nawrot & Blake, 1991) and intermittent presentation (ambiguous probes separated by brief interruptions, as in Pastukhov et al., 2013). The present results show that perceptual adaptation is influenced independently by the volume of adaptor and probe objects, but neither by the shape nor by the similarity between adaptor and probe objects.

General method

Observers

All participants had normal or corrected-to-normal vision. Apart from the authors, observers were naive as to the purpose of the experiments and were paid for their participation. Procedures were approved by the medical ethics board of the Otto-von-Guericke Universität, Magdeburg: "Ethik-Komission der Otto-von-Guericke-Universität an der Medizinischen Fakultät."

Apparatus

Stimuli were generated with MATLAB, using the Psychophysics Toolbox (Brainard, 1997). For Experiment 1, stimuli were displayed dichoptically using a mirror stereoscope in conjunction with an LCD screen (Eizo CG301W, www.eizo.com; resolution, 2,560 × 1,600 pixels; refresh, 60 Hz). The viewing distance was 87.5 cm, with one pixel subtending 0.014°. To facilitate binocular fusion, the main stimulus was surrounded by a checkerboard pattern. Observers responded using a gamepad (Logitech F310, logitech.com).

For Experiments 2–4, stimuli were displayed on a CRT screen (Iiyama VisionMaster Pro 514, iiyama.com; resolution, 1,600 × 1,200 pixels; refresh rate, 100 Hz). The viewing distance was 73 cm, so that each pixel subtended approximately 0.019°. Observers responded using a keyboard. In all experiments; background luminance was kept at 36 cd/m^2. The experimental room was dimly lit (ambient luminance at 80 cd/m^2).

The measure of aftereffect strength: probability of survival

As a measure of the aftereffect strength, we used the probability P_{survival} of a probe object appearing to rotate in the same direction as the preceding adaptor object. In Experiments 2–4, an object presented on a trial i was labeled as the *adaptor*, and one presented on a following trial $i + 1$ as the *probe*.

Values of P_{survival} below .5 indicate a negative aftereffect (probe tending to rotate in opposite direction), whereas values above .5 reveal facilitatory priming (probe tending to rotate in the same direction as adaptor). Note that values near .5 are difficult to interpret, since they may indicate either the complete absence of aftereffects or the cancellation of positive and negative aftereffects.

Here, we focus on relative rather than on absolute strengths of negative aftereffects. Typically, we compared aftereffects $P_{\text{surivival}}(X_1,X_2)$ obtained for one object pair (X_1,X_2) with aftereffects $P_{\text{surivival}}(Y_1,Y_2)$ obtained for another object pair (Y_1,Y_2).

Statistical methods

Valid trials were associated with a single response (i.e., we disregarded trials with no or multiple responses), indicating which of the two possible appearances the observer had perceived. Accordingly, we analyzed response distributions in terms of binomial statistics. For pairwise comparisons, we determined the probability that true difference of binomial proportions is zero, using the "Accurate Confidence Intervals" toolbox (see MATLAB central file exchange and Ross, 2003).

We included observer identity as an independent factor in analyses of variance (ANOVAs). This focuses the analysis on relative effects within individual observers. Such relative effects can be masked by absolute differences between observers. Including observers as an independent factor in the analysis solves this issue and ensures that shape-dependent effects are not driven by idiosyncrasies of individual observers.

Experiment 1: Adaptation to disambiguated displays

The first experiment assessed the extent to which perceptual adaptation to SFM is shape specific. Our aim was to extend the original study by Nawrot and Blake (1991) by employing a much wider range of shapes. We were particularly keen to know whether the similarity between adapted and tested shapes would prove important. To this end, we chose an ordered set of shapes, in which each shape "contained" all subsequent shapes: sphere, quad band, dual band, and single band (see Fig. 1a and Movies 1–4). Since any two could be transformed into each other by adding or subtracting "bands," the number of additions or subtractions separating two shapes provided a straightforward *dissimilarity* index. The dissimilarity index was defined by assigning an integer to each shape (1 to single band, 2 to dual band, 3 to quad band, 4 to sphere) and by forming the absolute value of the difference for any two shapes (see Pastukhov et al., 2013). In a companion publication, we have used the same set of shapes to probe the specificity of sensory memory (Pastukhov et al., 2013).

The experimental procedure followed that of Nawrot and Blake (1991): An *unambiguous* adaptor and a *fully ambiguous* probe were separated by a brief blank interval (see Fig. 1b). As in our earlier work on sensory memory (Pastukhov et al., 2013), we presented all possible shape pairs to establish the contingency of the adaptation aftereffect.

On the basis of prior work, we entertained two alternative working hypotheses. On the one hand, if aftereffects do not depend on the identities of adaptor and probe objects (as is suggested by the results of Nawrot & Blake, 1991), all object pairs should exhibit negative aftereffects of comparable strength (similar values of survival probability). On the other hand, if the aftereffect does depend on the congruency of SFM shapes (as was reported for sensory memory by Pastukhov et al., 2013), identical or similar object pairs should exhibit stronger aftereffects than dissimilar object pairs ($P^{\text{same}}_{\text{survival}} < P^{\text{different}}_{\text{survival}}$).

Method

Five observers (3 females, 2 males), including the first and second authors, participated in this experiment.

SFM stimuli consisted of 500 dots distributed randomly over the surface of four objects: sphere, quad band, dual band, and single band (see Fig. 1a and Movies 1–4). All objects measured 3.5° in height and rotated at 0.2 Hz.

The adaptor object was disambiguated with disparity and perspective cues. To introduce disparity, the objects presented to each eye were rotated about the z-axis by 1° relative to each other. To introduce perspective cues, dot size decreased linearly with depth (range, 0.1°–0.007°). The probe object was fully ambiguous: Dots were presented at identical positions to both eyes and had the same size (0.04°). Dot luminance was 110 cd/m^2.

A single trial (Fig. 1b) consisted of a random delay interval (0.5–1 s), an adaptor object (T_{prime}, = 10 s), a blank interval (T_{blank} = 0.4 s), a probe object (T_{probe} = 1 s), and a response

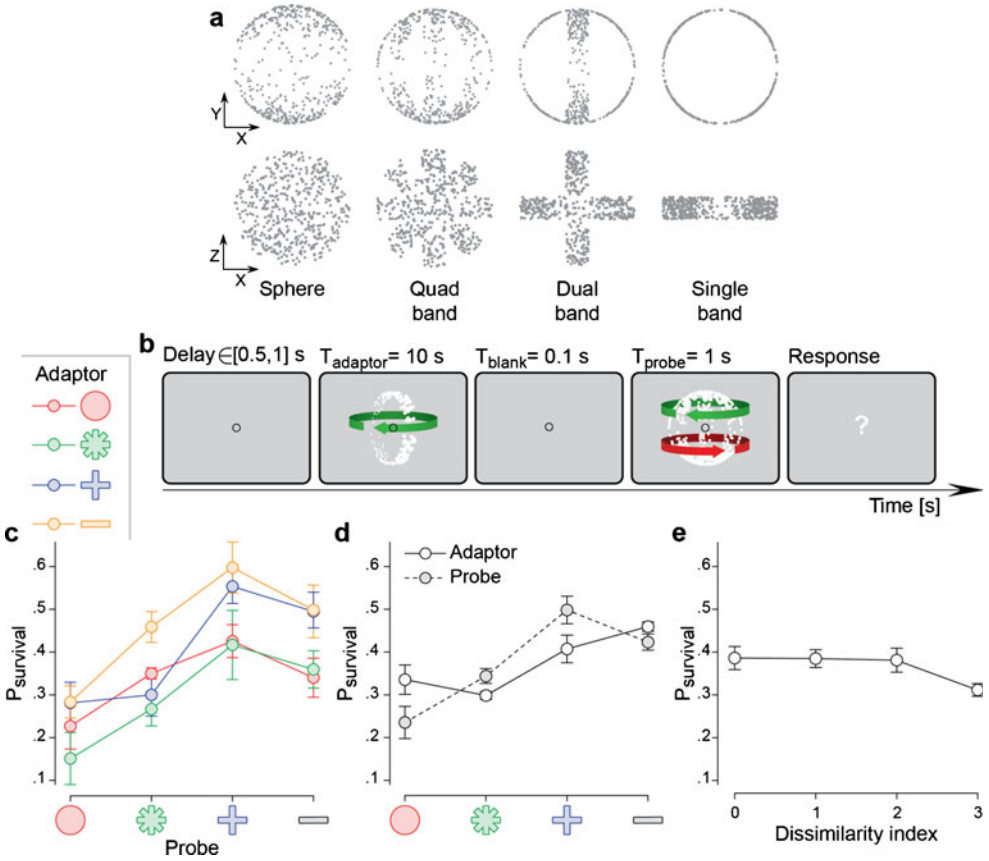

Fig. 1 Experiment 1: Adaptation to disambiguated displays. **a** Static snapshots of the stimuli used in the experiment, as seen on the screen (top row: front view, *x*–*y* plane) and as if viewed from above (bottom row: top view, *x*–*z* plane) (see Movies 1–4). **b** Schematic trial sequence: A variable delay interval (0.5–1 s) was followed by an adaptor object ($T_{adaptor}$ = 10 s), a blank interval (T_{blank} = 0.4 s), a probe object (T_{probe} = 1 s), and a response interval. **c** Probability $P_{survival}$ that adaptor and probe objects appeared to rotate in the same direction, for all possible pairs of shapes. **d** Average probability $P_{survival}$ as a function of the shape of the adaptor or probe object. **e** Average probability $P_{survival}$ as a function of dissimilarity index of two shapes (see the text for definition)

interval (average response time was 0.43 ± 0.09 s). The identities of adaptor and probe objects were chosen pseudorandomly, ensuring that all possible pairs appeared equally often.

A control experiment verified the effectiveness of the disambiguation. In this experiment, observers viewed the entire trial sequence but reported solely the apparent direction of rotation of the adaptor object. Intended and reported rotation differed on fewer than 2 % of the trials.

In the main experiment, observers reported the apparent direction of rotation of the *probe* object (using a gamepad). Specifically, they pressed *X* when the front surface appeared to rotate left, *B* when the front surface appeared to rotate right, and *A* when the apparent rotation reversed during the presentation. Approximately 10 % of the trials were discarded due to a reported reversal.

Results and discussion

The results of Experiment 1 revealed that object shape strongly influenced perceptual adaptation to the SFM shape (Fig. 1c). To disentangle the various possible dependencies, we performed a four-way ANOVA with Identity of adaptor object, Identity of probe object, and adaptor–probe congruency as independent factors. In addition, we included observer Identity as a fourth independent factor, so as to focus the analysis on differences between conditions (within each observer), rather than between observers.

The ANOVA showed a highly significant main effect of observer identity, $F(4, 68) = 15.8$, $p < .001$, adaptor identity, $F(3, 68) = 6.8$, $p = .0005$, and probe identity, $F(3, 68) = 16.5$, $p < 10^{-7}$), as is illustrated in Fig. 1d. Note that the latter two effects appeared to be correlated (we will return to this point later). Surprisingly, there was no significant effect of prime–probe congruency, $F(1, 68) = 0.21$, $p = .64$. The lack of any congruency effect was confirmed by the direct comparison of survival probabilities for object pairs with identical and different shapes: ($P^{same}_{survival} = .39 \pm .07$, $P^{different}_{survival} = .37 \pm .05$; $p = .45$, probability that true difference of binomial proportions $P^{different}_{survival} - P^{same}_{survival} = 0$). We also found no significant correlation between the shape dissimilarity index and strength of the negative aftereffect (Spearman rank correlation, $R = -.14$, $p = .22$; Fig. 1e).

These results demonstrate that perceptual adaptation to SFM does depend on object identity (specifically, object volume), extending the findings of an earlier report (Nawrot & Blake, 1991). Specifically, they show that the effect of perceptual adaptation depends on the identity of the adaptor object (with some shapes being better adaptors than other shapes), as well as on the identity of the probe object (with some shapes being better probes than others). Surprisingly, the results also show that the effect *does not* depend on whether adaptor and probe objects exhibit similar or dissimilar shapes. In this respect, the shape dependence of perceptual adaptation seems quite different from the shape dependence of sensory memory, which exhibits the exact opposite pattern of results (Pastukhov et al., 2013).

However, the different shape dependencies exhibited by perceptual adaptation, on the one hand, and by sensory memory, on the other hand, might reflect a simple stimulus difference: Perceptual adaptation was induced by unambiguous adaptor objects, whereas in our companion study, sensory memory was induced by fully ambiguous objects (Pastukhov et al., 2013). Our second experiment was designed to explore this possibility.

Experiment 2: Adaptation to fully ambiguous displays

To directly compare the respective shape dependencies of perceptual adaptation and of sensory memory, we used the experimental paradigm implemented in our companion study (Pastukhov et al., 2013). Fully ambiguous band shapes were presented intermittently (T_{on} = 2 s, T_{off} = 0.1 s) and in pseudorandom order, ensuring that all possible pairs of shapes succeeded each other equally often (Fig. 2a and Movie 5). Observers reported the apparent direction of rotation, with each object serving as a probe for the preceding object and as an adaptor for the subsequent one.

In contrast to long, blank intervals of the companion study (T_{off} = 1 s), here we interspersed short intervals (T_{off} = 0.1 s) with a mask stimulus (T_{mask} = 0.05 s). The mask was a yellow, uniform, filled sphere rotating around a horizontal axis (orthogonal to the vertical axis of rotation of the main stimulus). The point of using short intervals is to minimize recovery from adaptation, thus maximizing the strength of its negative aftereffect. The point of the masking stimulus is to terminate neural persistence, which otherwise strongly stabilizes perception (Klink et al., 2008; Kornmeier & Bach, 2004; Noest et al., 2007; Orbach et al., 1963; Pastukhov & Braun, 2013b). Due to its orthogonal axis of rotation, the mask does not interact with the aftereffect of the adaptor (Nawrot & Blake, 1989; Pastukhov & Braun, 2013b). We have previously demonstrated that this procedure is highly effective in maximizing negative aftereffects (Pastukhov & Braun, 2013b).

Method

Ten observers (8 females, 2 males), including the first and second authors, participated in this experiment.

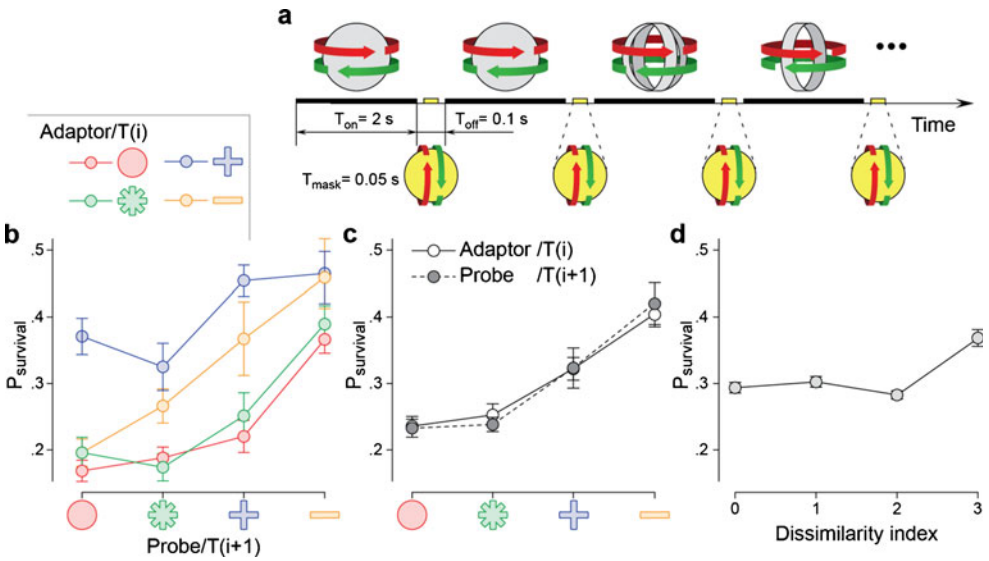

Fig. 2 Experiment 2: Adaptation to fully ambiguous displays, main group of 7 observers. **a** Schematic block sequence. Fully ambiguous SFM objects were presented intermittently (T_{on} = 2 s, T_{off} = 0.1 s) in pseudorandom order, ensuring that all shape pairs occur equally often. The T_{off} interval contained a yellow masking stimulus (see the text for details). Observers continuously reported on the perceived direction of rotation of the main stimulus. Each object served as a probe for the preceding object and as an adaptor for the subsequent one (see also Movie 5). **b** Probability $P_{survival}$ that adaptor [trial $T(i)$] and probe [trial $T(i + 1)$] objects appeared to rotate in the same direction, for all possible pairs of shapes. **c** Average probability $P_{survival}$ as a function of the shape of the adaptor or probe object. **d** Average probability $P_{survival}$ as a function of the dissimilarity index of two shapes (see the text for details)

SFM objects were identical to those used in Experiment 1, except that all shapes measured 5.7° in height and that dot diameter was uniformly 0.057°. SFM objects were fully ambiguous, and no disparity or size cues were used. Thus, the displays exactly matched the displays of the companion study of sensory memory (Pastukhov et al., 2013).

SFM objects were presented intermittently (T_{on} = 2 s, T_{off} = 0.1 s), with a mask object (T_{mask} = 0.05) appearing in the middle of the T_{off} interval (see Fig. 2a and Movie 5). The mask object was a filled sphere (identical to the one used in Experiment 3) that rotated about the horizontal axis. The main stimuli rotated about the vertical axis. This mask object disrupted neural persistence, revealing the full effect of perceptual adaption on the subsequent SFM object (Pastukhov & Braun, 2013b). To further distinguish it from the main stimuli, the mask stimulus was colored yellow.

A single block consisted of 120 T_{on} and 120 T_{off} intervals. SFM objects were presented in pseudorandom order, such as to ensure that all possible pairings of shapes occurred equally often. The probability that same shape appeared both during presentation i and presentation i + lag was approximately .25 for all lag values (t-test for mean of distribution μ = 0.25, $p > .05$). Randomized sequences were identical to those used in the companion study (Pastukhov et al., 2013).

Observers reported the perceived direction of illusory rotation using arrow keys. They also had the option of pressing the *down* key in case of an unclear/mixed perception. Trials with mixed responses, multiple responses, or no responses were excluded from the analysis (~1.4 %).

Results and discussion

A preliminary analysis revealed that observers exhibited two qualitatively different patterns of results, which we will present separately.

The main group, which comprised 7 out of 10 observers, replicated almost exactly the results of Experiment 1 (Fig. 2b–d). The overall priming effect was negative ($P^{same}_{survival}$=.29±.04, $P^{different}_{survival}$=.31±.05) and comparable for object pairs with identical and with different shapes (p = .43, probability that true difference of binomial proportions $P^{different}_{survival} - P^{same}_{survival} = 0$). A four-way ANOVA—with adaptor identity (trial i), probe identity (trial i + 1), adaptor–probe congruency, and observer identity as independent factors—revealed highly significant main effects of adaptor identity, $F(3, 98) = 17.4$, $p < 10^{-8}$, probe identity, $F(3, 98) = 22.3$, $p < 10^{-10}$, and observer identity, $F(6, 98) = 24$, $p < .001$, but no significant effect of adaptor–probe congruency, $F(1, 98) = 0.4$, $p = .53$. Again, we found no correlation between the dissimilarity index (see Experiment 1 for details) and the strength of negative aftereffects (Fig. 2d; Spearman rank correlation, $R = .16$, $p = .08$). Thus, this pattern of results is general in the sense that it applies both to disambiguated and to fully ambiguous adaptor objects.

The smaller subgroup (Fig. 3), comprising 3 out of 10 observers, produced a pattern of results similar to the companion study on sensory memory (Pastukhov et al., 2013). The overall priming effect was less negative ($P_{survival}$ = .42 ± .03), and $P_{survival}$ was higher for object pairs with identical shapes ($P^{same}_{survival}$ = .52 ±. 1, $P^{different}_{survival}$ = .39 ± .03; p = .054, probability that true difference of binomial proportions $P^{different}_{survival} - P^{same}_{survival} = 0$). The four-way ANOVA (same factors as for the main group) revealed a highly significant effect of adaptor–probe congruency, $F(1, 38) = 10.1$, $p = .003$, and of observer identity, $F(2, 38) = 6.9$, $p = .003$, but no effect of either adaptor identity, $F(3, 38) = 1.67$, $p = .19$, or probe identity, $F(3, 38) = 1.8$, $p = .16$. The dissimilarity index was significantly correlated with the strength of the aftereffect in a manner consistent with a *positive* aftereffect (Fig. 3c; $R = -.34$, $p = .018$) as reported in our earlier study (Pastukhov et al., 2013). In other words, more similar shapes produced higher perceptual stability.

In summary, whereas the main group of observers exhibited mostly negative priming consistent with perceptual adaptation, a smaller subgroup exhibited an interaction

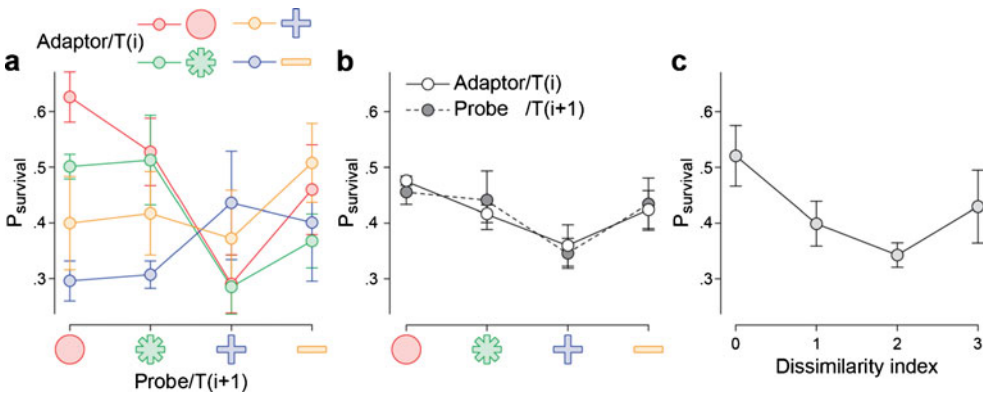

Fig. 3 Experiment 2: Adaptation to fully ambiguous displays, smaller group of three observers. **a** Probability $P_{survival}$ that adaptor and probe objects appeared to rotate in the same direction, for all possible pairs of shapes. **b** Average probability $P_{survival}$ as a function of the shape of the adaptor or probe object. **c** The negative correlation between $P_{survival}$ and dissimilarity index was significant (Spearman rank correlation, $R = -.34$, $p = .018$): Average probability $P_{survival}$ as a function of the dissimilarity of two consecutive shapes (see the text)

between negative and positive priming effects. The additional positive priming could have reflected sensory memory, especially since the results were qualitatively similar to those of the companion study (Pastukhov et al., 2013). Alternatively, the positive priming could also have been a manifestation of neural persistence (Pastukhov & Braun, 2013b), which may not have been masked completely for this group of observers.

Experiment 3: Volumetric properties

The third experiment combined hollow and solid SFM objects to ascertain whether or not perceptual adaptation is specific to volumetric properties. Hollow objects were composed exclusively by surface dots (hollow sphere, Movie 1; hollow cylinder, Movie 6), whereas solid objects comprised dots distributed throughout their volume (filled sphere, Movie 7; filled cylinder Movie 8). These SFM objects were identical to those used in the companion study (Pastukhov et al., 2013) that demonstrated that sensory memory is specific to volumetric properties. The procedure was identical to that in Experiment 2.

Method

Six observers (4 females, 2 males) participated in this experiment.

SFM stimuli consisted of 500 dots distributed randomly over the surfaces of two shapes (hollow sphere, Movie 1; hollow cylinder, Movie 6) or throughout the volume of two shapes (filled sphere, Movie 7; filled cylinder, Movie 8). All objects measured 5.7° in height, and the diameter of the individual dots was 0.057°. The stimuli were identical to those of Experiment 3 in the companion study (Pastukhov et al., 2013).

The procedure was identical to that of Experiment 2. Presentations with no response, multiple responses, or a mixed response were excluded from the analysis (~1.5 %).

Results and discussion

The results revealed a significant effect of volumetric properties, but no effect of adaptor–probe congruency, on the strength of perceptual adaptation (Fig. 4). A seven-way ANOVA was performed with the following independent factors: adaptor fill (hollow or solid), probe fill, adaptor shape (sphere or cylinder), probe shape, shape congruency, fill congruency, and observer identity. The results are summarized in Table 1. The only significant factor proved to be adaptor fill.

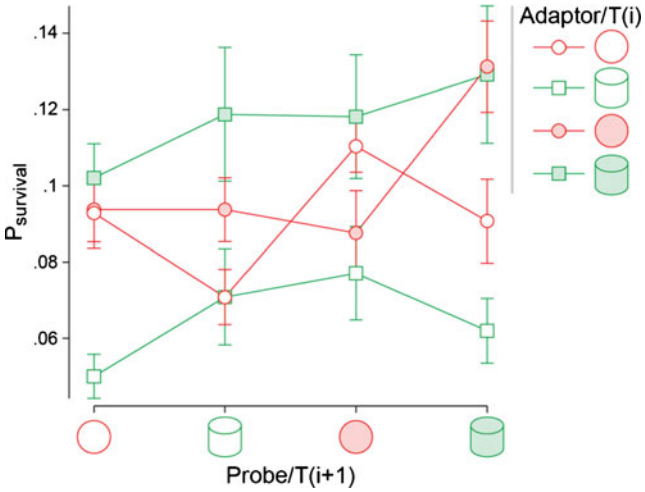

Fig. 4 Experiment 3: Volumetric properties and probability $P_{survival}$ that adaptor and probe objects appeared to rotate in the same direction

Experiment 4: Various shapes

The fourth experiment combined a variety of different objects in order to further investigate whether or not perceptual adaptation is specific to shape. A secondary purpose was to complete the comparison with the companion study (Pastukhov et al., 2013) of sensory memory, which had also investigated these shapes. The procedure was identical to that in Experiments 2 and 3.

Method

Six observers (4 females, 2 males), including the second author, participated in this experiment. SFM objects consisted of 500 dots distributed randomly over the surfaces of three shapes (hourglass, spinning top, and bent band) or throughout the volume of a fourth shape (tilted cross) (see Fig. 5a and Movies 9–12). All objects measured 5.7° in height, and the diameter of the individual dots was 0.057°. The stimuli were identical to those of Experiment 1 in the companion study (Pastukhov et al., 2013).

Table 1 Experiment 3: Results of seven-way ANOVA

Factor	*F*	*p*
Adaptor fill	13.7	.0004
Probe fill	2.82	.1
Adaptor shape	0.41	.53
Probe shape	0.27	.6
Fill congruency	0	.97
Form congruency	0.22	.64
Observer identity	12	<.001

Note. The only significant factor was adaptor fill. The degrees of freedom were 5/84 for observer identity, 1/84 for all other factors

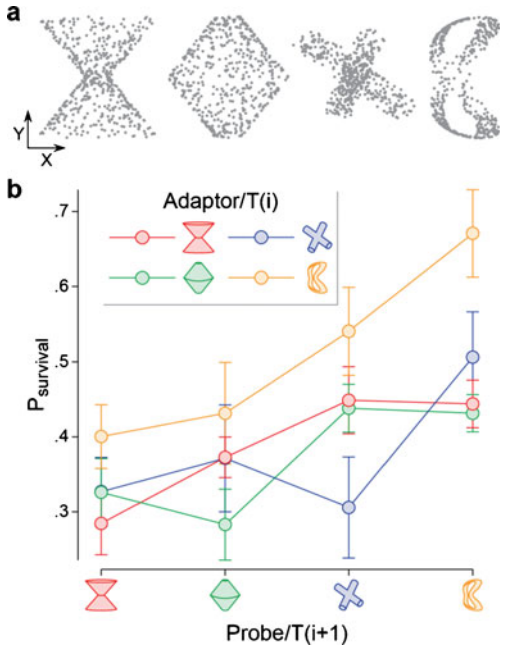

Fig. 5 Experiment 4: Various shapes. **a** Static snapshots of the stimuli used in the experiment, as seen on the screen (front view, x–y plane) (see also Movies 9–12). In the main text, these stimuli are termed *hourglass*, *spinning top*, *tilted cross*, and *bent band* (from left to right). **b** Probability P_{survival} that adaptor and probe objects appeared to rotate in the same direction

The procedure was identical to that of Experiments 2 and 3. Presentations with no response, multiple responses, or a mixed response were excluded from the analysis (~1.5 %).

Results and discussion

The results were fully consistent with outcome of the preceding experiments. Perceptual adaptation depended on the identity of adaptor and probe objects, but not on their similarity (Fig. 5b). A four-way ANOVA with adaptor identity, probe identity, adaptor–probe congruency, and observer identity as independent factors revealed highly significant main effects of adaptor identity, $F(3, 83) = 5.1$, $p = .003$, probe identity, $F(3, 83) = 7.3$, $p < .0002$, and observer identity, $F(5, 83) = 3.2$, $p = .01$, but no effect of adaptor–probe congruency, $F(1, 83) = 0\ .98$, $p = .33$.

Combined analysis

The purpose of the combined analysis was to establish feature selectivity of an adapting population and to compare it with properties of various neural representations involved in the processing of SFM. Before we proceed with a detailed analysis, we define various measures for the relation between object shapes and the strength of aftereffects.

Definitions

We assume that SFM objects stimulate subsets of retinotopically and/or spatiotopically organized neuronal populations that are selective for local velocity in the image plane and/or in three-dimensional space. For simplicity, we conflate these two possibilities and formulate the argument in terms of three-dimensional volumes.

To estimate which part of such a population a given SFM object stimulates, we mapped each object onto a rectangular grid of voxels with linear size 0.05 (unity being the height of each SFM object). Each voxel represents a neural unit with a receptive field centered at a particular image location (x-, y-coordinate) and depth plane (z-coordinate). Note that a given voxel always experienced the same image velocity, since all SFM objects rotated with the same angular velocity. A voxel assumed a value of unity if it contained at least one dot of the SFM object. All other voxels assumed values of zero.

The total number of stimulated voxels was termed the *occupied volume*. It estimates which subset of a spatially distributed representation is engaged by SFM object A:

$$Occupied\,volume\,(\mathrm{A}) = \sum V_A. \tag{1}$$

Because occupied volume is expressed in arbitrary units, we defined it as a fraction of the largest occupied volume (filled cylinder). *Summed volume* occupied by two objects was computed as a simple sum of two individual occupied volumes:

$$Summed\,volume\,(\mathrm{A},\mathrm{B}) = \sum V_A + \sum V_B. \tag{2}$$

Several measures were used to describe the relation between two SFM objects. *Absolute overlap* was defined as the intersection or, equivalently, as the product of two volume maps V_{A} and V_{B}:

$$V_A \cap V_B = \sum V_A \cdot V_B. \tag{3}$$

The *combined volume* was defined as the union of two volume maps or, equivalently, as the number of nonzero voxels in the sum of both maps:

$$V_A \cup V_B = \sum (V_A + V_B) > 0. \tag{4}$$

Relative overlap between volumes V_{adaptor} and V_{probe} was defined as the ratio between the overlapping volume and the probe volume:

$$Relative\,overlap\left(V_{adaptor}, V_{probe}\right) = \frac{V_{adaptor} \cap V_{probe}}{V_{probe}}. \tag{5}$$

Finally, *symmetric overlap* of volumes $V_{adaptor}$ and V_{probe} was defined as the ratio between overlap and combined volume:

$$Symmetric\,overlap\left(V_{adaptor}, V_{probe}\right) = \frac{V_{adaptor} \cap V_{probe}}{V_{adaptor} \cup V_{probe}}. \quad (6)$$

In a similar spirit, we defined several measures to describe experimentally observed interaction between two SFM objects. *Relative priming* was defined as the strength of the negative aftereffect induced by an adaptor object on the probe:

$$Relative\,priming(\mathrm{A}, \mathrm{B}) = P_{survival}(A, B). \quad (7)$$

Note that relative priming is a *directional* measure, since the presentation order of two objects is important.

Symmetric priming was defined as the strength of the negative aftereffect induced by one object on another, irrespective of their presentation order:

$$Symmetric\,priming(\mathrm{A}, \mathrm{B}) = \frac{P_{survival}(A, B) + P_{survival}(B, A)}{2}. \quad (8)$$

All correlation coefficients in this section were computed using the Spearman rank correlation.

Different neural levels of SFM representation

Neurophysiological evidence indicates that SFM objects elicit responses at multiple levels of the visual cortex (see Orban, 2011, for a comprehensive review). Initially, local dot motion drives direction-selective units in low-level, retinotopically organized areas of the visual cortex, such as area V1 or V2 (Livingstone & Hubel, 1988; Sincich & Horton, 2005). This information is then passed to intermediate-level cortical areas, such as area MT (Movshon & Newsome, 1996; Rust, Mante, Simoncelli, & Movshon, 2006), which contain velocity-selective and speed-gradient-selective neurons with much larger receptive fields (Martinez-Trujillo et al., 2005; Rust et al., 2006). At a third level, this information is integrated by neurons with even larger receptive fields, which are selective for complex motion flows, such as rotation or expansion. The likely cortical locations of these neurons are higher areas of the dorsal path, such as areas MT/V5 (Bradley, Chang, & Andersen, 1998), MST (Morrone, Burr, & Vaina, 1995; Smith, Wall, Williams, & Singh, 2006; K. Tanaka, Fukada, & Saito, 1989), or regions in the intraparietal sulcus (Orban et al., 2003; Peuskens et al., 2004). Given the disparate selectivities, adaptation at each of these three levels would be expected to produce different patterns of results. Below, we formulate these expectations and compare them with our empirical observations.

Predictions for low-level, retinotopically organized representations are presented in Fig. 6. Here, the negative aftereffect should be maximal when adaptor and probe objects engage the same units and minimal when they engage different units. In other words, strength of a negative aftereffect, expressed in terms of *relative priming*, should correlate with *relative overlap* (as defined above). Moreover,

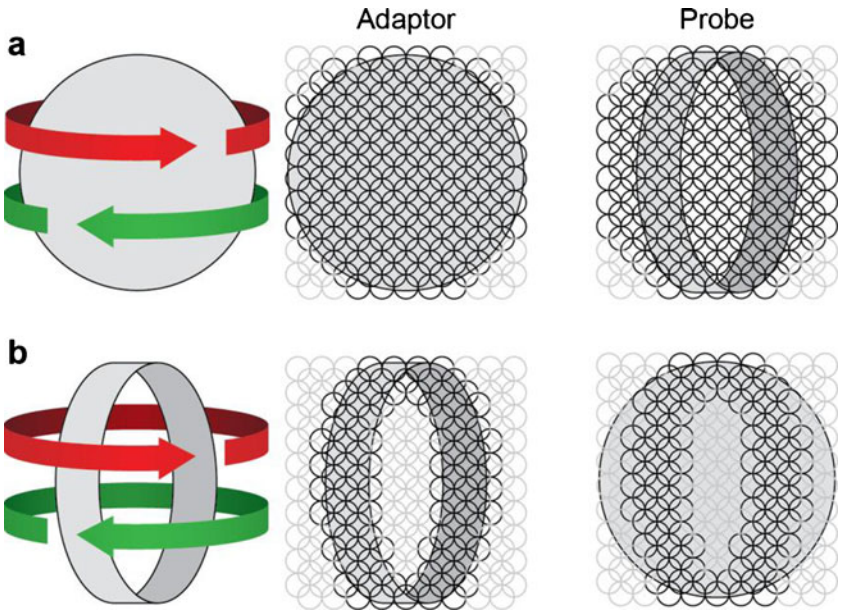

Fig. 6 Hypothetical adapting population of local, motion-selective units that tile visual space: Structure-from-motion object and subpopulations engaged by adaptor and probe objects. **a** A large adaptor (e.g., sphere) engages and adapts a large fraction of the population (darker circles). A subsequent, smaller probe (e.g., band) engages only adapted units, resulting in a large aftereffect. **b** A smaller adaptor (e.g., band) engages and adapts a small fraction of the population (darker circles). A subsequent, larger probe (e.g., sphere) engages both adapted and unadapted units, resulting in a smaller aftereffect. In general, aftereffect strength would depend on object order

negative aftereffects should depend on object order. For example, a sphere followed by a band should produce a much larger aftereffect (Fig. 6a; relative overlap = 1) than a band followed by a sphere (Fig. 6b; relative overlap << 1). However, we find no significant correlation between relative overlap and relative priming, $R = -.132$, $p = .29$. The clear implication is that neural adaptation in low-level, retinotopic populations of neurons tiling visual space (such as areas V1 and V2) does not contribute substantially to the negative aftereffects observed in this study.

Adaptation in intermediate-level populations, where neurons have larger receptive fields and are selective for velocity and speed gradients, would be expected to be specific to the velocity profile of adaptor and probe objects. Object pairs with similar distributions of velocities should produce stronger aftereffects than should objects with dissimilar velocities. To test for this possibility, we converted the distribution of z-coordinates of a given volume map into a distribution of planar velocities and of speed gradients. Next, we used these distributions to compute relative overlap in velocity and speed gradient space (rather than visual space). We found no significant correlation between either relative priming and relative overlap in velocity space, $R = -.018$, $p = .88$, or relative priming and relative overlap in speed gradient space, $R = -.17$, $p = .17$. Similarly, we found no significant correlation between symmetric priming and either the statistical similarity (computed by Wilcoxon rank-sum test) of the two velocity distributions, $R = -.019$, $p = .88$, or the statistical similarity of the two speed gradient distributions, $R = -.11$, $p = .4$. Thus, it seems unlikely that perceptual adaptation at the level of velocity-selective or speed-gradient-selective neurons contributes substantially to the negative aftereffects observed in this study.

Finally, adaptation at the higher level is expected to be specific to the complex motion flows, but not to the shape of adaptor and probe objects, because the receptive fields at this level are much larger than our SFM objects (Desimone & Ungerleider, 1986; Raiguel et al., 1997; Van Essen, Maunsell, & Bixby, 1981). Similarly, it should not be specific for velocity distribution, since any information about component velocities is expected to be lost in the computation of the global rotation. This prediction—selectivity for overall rotation in depth but not for any specifics of object shape—agrees well with our results. Indeed, negative aftereffects did not differ significantly when objects were congruent (similar) and when they were incongruent (dissimilar). This was true when each experiment was considered individually (see Figs. 1e and 2d) and when all four experiments were considered together ($p = .3$; probability that true difference of binomial proportions $P_{\text{survival}}^{\text{different}} - P_{\text{survival}}^{\text{same}} = 0$). Generally, all measures of object similarity in terms of volume, shape, or velocity profile consistently failed to predict negative aftereffects.

To summarize, the experimental paradigm investigated here produced no indication of neural adaptation at lower-level (location-specific) or intermediate-level (velocity-specific) representations. Instead, our results are consistent with neural adaptation of higher-level (rotation-specific) representations. Importantly, the adapting level does not seem to retain any details of object shape (other than overall rotation). This explains why negative aftereffects are insensitive to congruency or similarity between adaptor and probe objects.

Below, we further characterize the adapting representation by analyzing how negative aftereffects vary with single-object properties.

Dependence on object volume

In our experiments, effectiveness as an adaptor and sensitivity as a probe varied dramatically with individual object volume. We obtained strong and highly significant correlations both when an object served as an adaptor (Fig. 7a; Spearman rank correlation, $R = -.81$, $p < .0001$) and when it served as a probe (Fig. 7b) $R = -.85$, $p < .0001$. In both cases, the larger occupied volume led to the stronger negative aftereffect (lower values of P_{survival}). For the filled/hollow objects of Experiment 3, P_{survival} approached floor level ($P_{\text{survival}} = 0$) and, thus, may have underrepresented the true aftereffect. Moreover, in Experiments 1 and 2, we found that more effective adaptors also tended to be more sensitive probes (see Figs. 1d and 2b). The correlation between *effectiveness* and *sensitivity* became even more evident when all four experiments were considered together, as illustrated in Fig. 7c. The linear Pearson's correlation between the average probability $P_{\text{survival}}(\text{A}\rightarrow\text{X})$, when object A serves as an adaptor, and the average probability $P_{\text{survival}}(\text{X}\rightarrow\text{A})$, when object A serves as a probe, was highly significant, $R = .95$, $p < 10^{-7}$.

To test the independence of adaptor and probe effects, we correlated summed volume and symmetric priming, obtaining a strong and highly significant relation, $R = -.86$, $p < 10^{-17}$. In essence, this means that the detrimental effect of smaller adaptors (such as a single band) can be compensated by the enhanced effect of larger probes (such as a sphere). To further examine individual influence of adaptor and probe on negative aftereffect, we slightly modified the formula to compute weighted summed volume:

$$\textit{Weighted summed volume}\,(\text{adaptor}, \text{probe}) = W \cdot \sum V_{adaptor} + \sum V_{probe}, \tag{9}$$

where the added coefficient W controls a relative contribution of two objects. Next, we used a linear optimization routine to find a value of W that maximized correlation between weighted summed volume and symmetric priming. Optimal

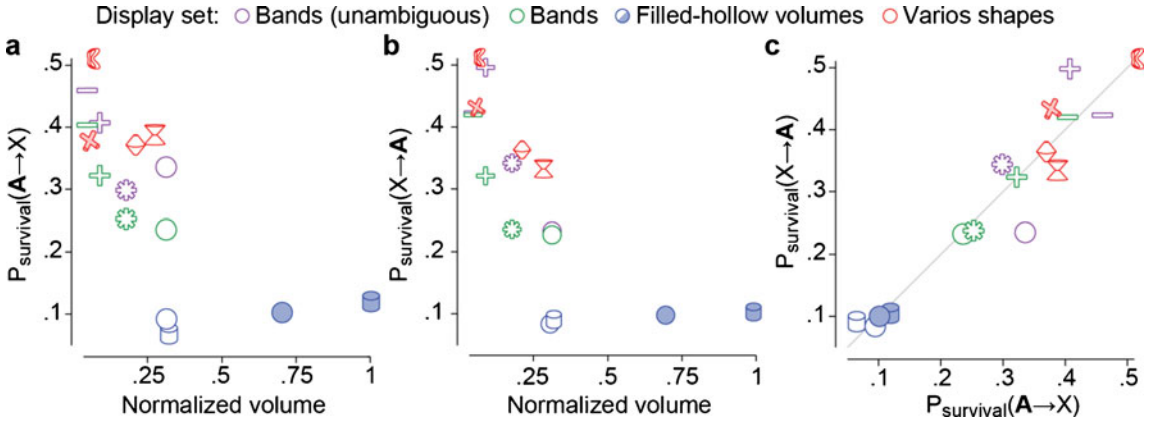

Fig. 7 Dependence of negative aftereffect on object volume. The object's effectiveness as an adaptor (**a**) and as a probe (**b**) increased with volume. Panel a: Average probability $P_{survival}$(A→X) as a function of the occupied volume of A. Panel b Average probability $P_{survival}$(X→A) as a function of the occupied volume of A. **c** An effective adaptor was also a sensitive probe. There was a correlation between the average probability $P_{survival}$(A→X) that the apparent rotation of a given adaptor A persists in any probe X and the average probability $P_{survival}$(X→A) that the apparent rotation of any adaptor X persists in a given probe A (Pearson correlation, $R = .95$, $p < 10^{-7}$)

value was $W = .52$, suggesting that probe volume might had a larger influence on strength of negative aftereffect, although the increase in correlation strength was minimal, $R = -.87$, $p < 10^{-18}$.

Taken together, these analyses suggest that negative aftereffects vary independently with the volumes of adaptor and probe objects.

An explanatory hypothesis

We are now in the position to account for all observations with a single explanatory hypothesis. The main difficulty is to reconcile the lack of shape specificity with the volume dependence of negative aftereffects. In addition, we need to take into account that perceptual adaptation primarily affects higher-level representations (rotation-in-depth), but not intermediate-level (velocity-selective) or low-level (direction-selective) representations (for the time scale used in the present study).

The key part of our hypothesis is that the volume dependence of (nonadapting) low- or intermediate-level representations is inherited by (adapting) higher-level representations in terms of stronger or weaker activity. In particular, we assume that the total volume of an SFM object determines the number of neurons that are stimulated in low- or intermediate-level representations (e.g., direction-selective neurons in areas V1/V2, and velocity- or speed-gradient-selective neurons in area MT; compare Fig. 6a and b). We further assume that more *numerous* activations at low and intermediate levels translate into *stronger* activations at the higher level. This is illustrated schematically in Fig. 8a and explains why larger objects are more effective adaptors: Stronger activation of the adapting representation produces "deeper" adaptation. The same mechanism also explains why larger objects are more sensitive probes (Fig. 8b): When an

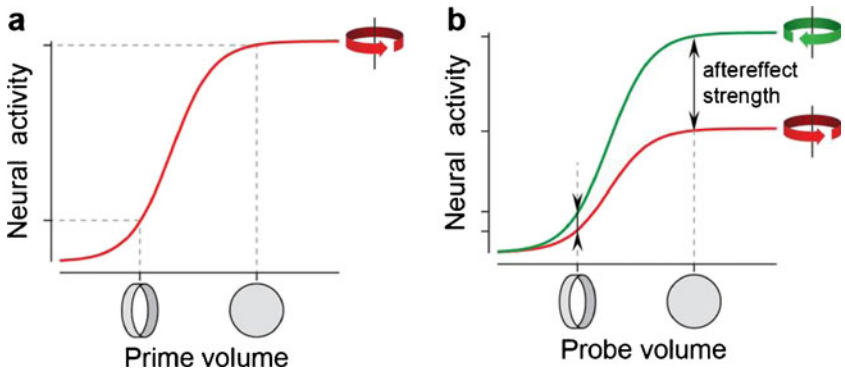

Fig. 8 Hypothetical link between volume of an SFM object, its effectiveness as an adaptor, and its sensitivity as a probe. **a** Large objects (e.g., sphere) lead to higher activity in the rotation representation. For this reason, large objects are more effective adaptors. The inverse is true for small objects (e.g., single band). **b** Differential activation of competing rotation-selective populations by a probe object. Large objects (sphere) will elicit more activity and, crucially, a greater activity difference between adapted and unadapted populations than will small objects (single band). For this reason, large objects are more sensitive probes

Table 2 Comparison between perceptual adaptation and sensory memory (Pastukhov et al., 2013)

	Perceptual Adaptation	Sensory Memory
Adaptor identity/attribute (ANOVA)		
Various shapes (identity)	***p* = .003**	p = .9,
Bands (identity)	***p* < .0001**	p = .61
Filled-hollow shapes (solidity)	***p* = .0004**	p = .16
Adaptor/probe volume (correlation)		
Adaptor volume vs. $P_{survival}$	***R* = −.81, *p* < .0001**	R = −.081, p = .8
Probe volume vs. $P_{survival}$:	***R* = −.85, *p* < .0001**	R = −.19, p = .56
Summed volume (correlation)		
V(adaptor) + V(probe) vs. $P_{survival}$(A,B)	***R* = −.86, *p* < .0001**	R = -.12, p = .41
Adaptor–probe congruency (ANOVA)		
Various shapes (identity)	p = .33	***p* < .0001**
Bands (identity)	p = .53	***p* < .0001**
Filled-hollow shapes (solidity)	p = .97	**p < .0001**
Adaptor–probe similarity		
Dissimilarity index vs. $P_{survival}$ (bands only):	R = .16, p = .08,	***R* = .76, *p* < .0001**
Symmetric overlap vs. symmetric priming	R = −.24, p = .06	***R* = .78, *p* < .0001**
$P_{survival}$(A,B) and $P_{survival}$(B,A) (Pearson correlation)	***R* = .663, *p* = .0004**	***R* = .97, *p* < .0001**

Note. Spearman rank correlations, unless specified otherwise. Bold font marks statistically significant results

(ambiguous) probe object differentially activates two competing representations of illusory rotation at the higher level (two curves in Fig. 8b), the strength of the aftereffect depends on the activity difference (arrows in Fig. 8b). Thus, larger probe objects would experience stronger aftereffects than would smaller probe objects (again due to stronger activation of the adapting representation).

Comparison with sensory memory in SFM

One of the purposes of our study was to compare and contrast shape selectivity of perceptual adaptation and sensory memory. Perceptual adaptation and sensory memory exhibit very different dependencies on the shape of SFM objects, as summarized in Table 2.

The companion study demonstrated that strength of sensory memory depended only on the similarity and congruency of prime and probe SFM objects (Pastukhov et al., 2013). Prime–probe congruency was consistently the most significant factor in ANOVA analyses, and perceptual stability was best correlated with symmetric overlap (Fig. 9a), R = .78, p < .0001. In contrast, there was no effect of the individual identity of prime or probe objects. Finally, there was no relationship between either the individual or the summed volumes of prime or probe objects and strength of sensory memory (Fig. 9c), R = −.12, p = .41.

Perceptual adaptation exhibited the opposite pattern of results, since it depended on the individual volume of prime and probe objects, but not on their similarity or congruency. There was no significant correlation between symmetric priming and symmetric overlap, R = −.24, p = .06. The relative success of object volume in predicting negative aftereffects is illustrated in Fig. 9d, R = −.86, p < .0001, whereas the relative failure of shape similarity is shown in Fig. 9b.

General discussion

Selective adaptation paradigms offer insight into the structure of underlying neural representations for both negative (Blakemore & Campbell, 1969; Leopold et al., 2001; Malach, 2012; Preston et al., 2009) and positive (Caplovitz et al., 2011; Feldman & Tremoulet, 2006; Kawachi et al., 2011; Kramer & Rudd, 1999; Kristjánsson & Campana, 2010; Pastukhov et al., 2013; Shechter et al., 1988; Yu, 2000) priming effects. In addition to characterizing the feature specificity of each such representation, the comparison of positive and negative priming effects yields further insight about the relation of the respective representations in question. Potentially, this approach can help to identify several distinct levels of processing. The present study investigated the shape selectivity of perceptual adaptation (negative history effect) to SFM displays (Nawrot & Blake, 1991), complementing our earlier study of sensory memory (positive history effect) in such displays (Pastukhov et al., 2013).

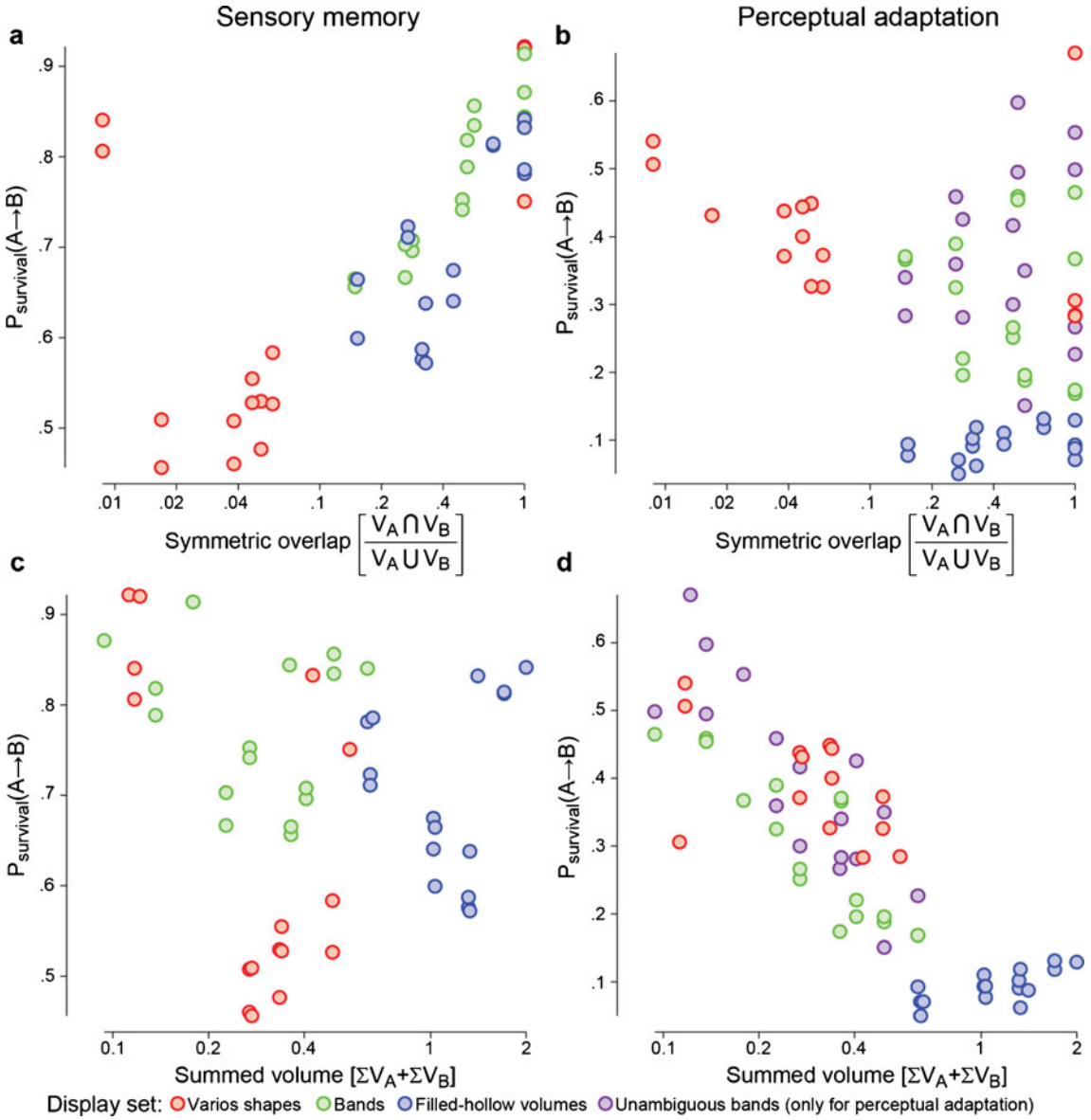

Fig. 9 Predictiveness of symmetric overlap and summed volume measures (Spearman rank correlation): $P_{survival}$ as a function of the symmetric overlap between adaptor and probe. **a** Sensory memory, $R = .78$, $p < 10^{-9}$ (excluding two outliers: $R = .9$, $p < 10^{-17}$). **b** Perceptual adaptation, $R = -.24$, $p = .06$. (**c**, **d**) $P_{survival}$ as a function of the summed volume occupied by an adaptor and a probe. Panel c: Sensory memory, $R = -.12$, $p = .41$. Panel d: Perceptual adaptation, $R = -.86$, $p < 10^{-17}$

Both studies investigated three-dimensional objects in their volume, their shape, and/or their solidity (hollow or filled). The present results demonstrated that the identities of both adaptor and probe objects modulate perceptual destabilization due to adaptation, extending an earlier report (Nawrot & Blake, 1991). Surprisingly, however, it was not the pairing of adaptor and probe objects that mattered (i.e., their pairwise congruency or similarity), but the separate identities of each object. The combined analysis of all experiments suggested that the key variable determining strength of adaptation was the volume occupied by each SFM object.

To reconcile strong volume dependence and lack of shape specificity, we propose that an adapting population at higher cortical levels (such as area MST) represents illusory rotation in depth but does not retain information about object shape. We further propose that the adapting representation is activated more strongly by larger than by smaller objects, since the former generate more feed-forward input from low- and intermediate-level representations (such as areas V1, V2, and MT). Indeed, the activation of single units in area MST is known to grow with stimulus size (Celebrini & Newsome, 1994; Duffy & Wurtz, 1991). Since stronger activation is expected to produce "deeper" adaptation, this

would explain why larger objects are both more effective adaptors and more sensitive probes than are smaller objects.

Finally, the pattern of results from perceptual adaptation was the opposite of that obtained from sensory memory (Pastukhov et al., 2013). Unlike perceptual adaptation, sensory memory reflects the similarity and congruency of prime and probe objects, but not their volumes (Table 2). Thus, the population maintaining sensory memory seems to represent abstract features of object shape, whereas the population maintaining perceptual adaptation represents abstract features of object motion in depth. These results demonstrate conclusively that positive and negative priming effects with SFM objects are mediated by distinct representations with disparate selectivities. Thus, at least in the experimental situations investigated here, negative and positive priming are *not* manifestations of a single neural mechanism, as has been proposed (Gepshtein & Kubovy, 2005; Noest et al., 2007; Noest & van Wezel, 2012). However, it is possible that such a single mechanism underpins positive and negative aftereffects associated with longer time scales (Brascamp et al., 2008; Brascamp et al., 2007; Brascamp et al., 2009).

Conclusions

To summarize, we report that volume of both adaptor and probe objects modulates negative aftereffect due to perceptual adaptation. However, the influence of two objects was independent, since any relationship between two shapes (such as overlap between volumes, similarity of shape, or similarity of velocity profiles) failed to modulate the negative aftereffect. This pattern of results was the opposite of that observed for sensory memory of SFM objects, suggesting that the two aftereffects engage distinct neural representations.

References

Adams, P. A. (1954). The effect of past experience on the perspective reversal of a tridimensional figure. *The American Journal of Psychology, 67*(4), 708–710.

Blakemore, C., & Campbell, F. W. (1969). On the existence of neurones in the human visual system selectively sensitive to the orientation and size of retinal images. *The Journal of Physiology, 203*(1), 237–260.

Bradley, D. C., Chang, G. C., & Andersen, R. A. (1998). Encoding of three-dimensional structure-from-motion by primate area MT neurons. *Nature, 392*(6677), 714–717. doi:10.1038/33688

Brainard, D. H. (1997). The Psychophysics Toolbox. *Spatial Vision, 10*(4), 433–436. doi:10.1163/156856897X00357

Brascamp, J. W., Kanai, R., Walsh, V., & van Ee, R. (2010). Human middle temporal cortex, perceptual bias, and perceptual memory for ambiguous three-dimensional motion. *Journal of Neuroscience, 30*(2), 760–766. doi:10.1523/JNEUROSCI.4171-09.2010

Brascamp, J. W., Knapen, T. H. J., Kanai, R., Noest, A. J., van Ee, R., & van den Berg, A. V. (2008). Multi-timescale perceptual history resolves visual ambiguity. *PloS One, 3*(1), e1497. doi:10.1371/journal.pone.0001497

Brascamp, J. W., Knapen, T. H. J., Kanai, R., van Ee, R., & van den Berg, A. V. (2007). Flash suppression and flash facilitation in binocular rivalry. *Journal of Vision, 7*(12), 12.1–12. doi:10.1167/7.12.12

Brascamp, J. W., Pearson, J., Blake, R., & van den Berg, A. V. (2009). Intermittent ambiguous stimuli: Implicit memory causes periodic perceptual alternations. *Journal of Vision, 9*(3), 3.1–23. doi:10.1167/9.3.3

Caplovitz, G. P., Shapiro, A. G., & Stroud, S. (2011). The maintenance and disambiguation of object representations depend upon feature contrast within and between objects. *Journal of Vision, 11*(14), 1–14. doi:10.1167/11.14.1

Celebrini, S., & Newsome, W. T. (1994). Neuronal and psychophysical sensitivity to motion signals in extrastriate area MST of the macaque monkey. *The Journal of Neuroscience: The Official Journal of the Society for Neuroscience, 14*(7), 4109–4124.

Chen, X., & He, S. (2004). Local factors determine the stabilization of monocular ambiguous and binocular rivalry stimuli. *Current Biology, 14*(11), 1013–1017. doi:10.1016/j.cub.2004.05.042

Clifford, C. W. G., Webster, M. A., Stanley, G. B., Stocker, A. A., Kohn, A., Sharpee, T. O., & Schwartz, O. (2007). Visual adaptation: Neural, psychological and computational aspects. *Vision Research, 47*(25), 3125–3131. doi:10.1016/j.visres.2007.08.023

Daelli, V., van Rijsbergen, N. J., & Treves, A. (2010). How recent experience affects the perception of ambiguous objects. *Brain Research, 1322,* 81–91. doi:10.1016/j.brainres.2010.01.060

De Jong, M. C., Knapen, T. H. J., & van Ee, R. (2012). Opposite influence of perceptual memory on initial and prolonged perception of sensory ambiguity. *PloS One, 7*(1), e30595. doi:10.1371/journal.pone.0030595

De Jong, M. C., Kourtzi, Z., & van Ee, R. (2012). Perceptual experience modulates cortical circuits involved in visual awareness. *The European Journal of Neuroscience, 36*(12), 3718–3731. doi:10.1111/ejn.12005

Desimone, R. (1996). Neural mechanisms for visual memory and their role in attention. *Proceedings of the National Academy of Sciences of the United States of America, 93*(24), 13494–13499.

Desimone, R., & Ungerleider, L. G. (1986). Multiple visual areas in the caudal superior temporal sulcus of the macaque. *The Journal of Comparative Neurology, 248*(2), 164–189. doi:10.1002/cne.902480203

Duffy, C. J., & Wurtz, R. H. (1991). Sensitivity of MST neurons to optic flow stimuli. II. Mechanisms of response selectivity revealed by small-field stimuli. *Journal of Neurophysiology, 65*(6), 1346–1359.

Fang, F., Murray, S. O., & He, S. (2007). Duration-dependent FMRI adaptation and distributed viewer-centered face representation in human visual cortex. *Cerebral Cortex (New York, N.Y.: 1991), 17*(6), 1402–1411. doi:10.1093/cercor/bhl053

Feldman, J., & Tremoulet, P. D. (2006). Individuation of visual objects over time. *Cognition, 99*(2), 131–165. doi:10.1016/j.cognition.2004.12.008

Ganel, T., Gonzalez, C. L. R., Valyear, K. F., Culham, J. C., Goodale, M. A., & Köhler, S. (2006). The relationship between fMRI adaptation and repetition priming. *NeuroImage, 32*(3), 1432–1440. doi:10.1016/j.neuroimage.2006.05.039

Gepshtein, S., & Kubovy, M. (2005). Stability and change in perception: Spatial organization in temporal context. *Experimental Brain Research., 160*(4), 487–495. doi:10.1007/s00221-004-2038-3

Gigante, G., Mattia, M., Braun, J., & Del Giudice, P. (2009). Bistable perception modeled as competing stochastic integrations at two levels. *PLoS Computational Biology, 5*(7), e1000430. doi:10.1371/journal.pcbi.1000430

Grill-Spector, K., Henson, R., & Martin, A. (2006). Repetition and the brain: Neural models of stimulus-specific effects. *Trends in Cognitive Sciences, 10*(1), 14–23. doi:10.1016/j.tics.2005.11.006

Grill-Spector, K., Kushnir, T., Edelman, S., Avidan, G., Itzchak, Y., & Malach, R. (1999). Differential processing of objects under various viewing conditions in the human lateral occipital complex. *Neuron, 24*(1), 187–203. doi:10.1016/S0896-6273(00)80832-6

Huk, A. C., & Heeger, D. J. (2002). Pattern-motion responses in human visual cortex. *Nature Neuroscience, 5*(1), 72–75. doi:10.1038/nn774

Kawachi, Y., Kawabe, T., & Gyoba, J. (2011). Stream/bounce event perception reveals a temporal limit of motion correspondence based on surface feature over space and time. *i-Perception, 2*(5), 428–439. doi:10.1068/i0399

Klink, P. C., van Ee, R., Nijs, M. M., Brouwer, G. J., Noest, A. J., & van Wezel, R. J. A. (2008). Early interactions between neuronal adaptation and voluntary control determine perceptual choices in bistable vision. *Journal of Vision, 8*(5), 16.1–18. doi:10.1167/8.5.16

Kornmeier, J., & Bach, M. (2004). Early neural activity in Necker-cube reversal: Evidence for low-level processing of a gestalt phenomenon. *Psychophysiology, 41*(1), 1–8. doi:10.1046/j.1469-8986.2003.00126.x

Kornmeier, J., Ehm, W., Bigalke, H., & Bach, M. (2007). Discontinuous presentation of ambiguous figures: How interstimulus-interval durations affect reversal dynamics and ERPs. *Psychophysiology, 44*(4), 552–560. doi:10.1111/j.1469-8986.2007.00525.x

Kramer, P., & Rudd, M. (1999). Visible persistence and form correspondence in Ternus apparent motion. *Perception & Psychophysics, 61*(5), 952–962. doi:10.3758/BF03206909

Kristjánsson, A., & Campana, G. (2010). Where perception meets memory: A review of repetition priming in visual search tasks. *Attention, Perception & Psychophysics, 72*(1), 5–18. doi:10.3758/APP.72.1.5

Leopold, D. A., O'Toole, A. J., Vetter, T., & Blanz, V. (2001). Prototype-referenced shape encoding revealed by high-level aftereffects. *Nature Neuroscience, 4*(1), 89–94. doi:10.1038/82947

Leopold, D. A., Wilke, M., Maier, A., & Logothetis, N. K. (2002). Stable perception of visually ambiguous patterns. *Nature Neuroscience, 5*(6), 605–609. doi:10.1038/nn851

Livingstone, M., & Hubel, D. (1988). Segregation of form, color, movement, and depth: Anatomy, physiology, and perception. *Science (New York, N.Y.), 240*(4853), 740–749. doi:10.1126/science.3283936

Maier, A., Wilke, M., Logothetis, N. K., & Leopold, D. A. (2003). Perception of temporally interleaved ambiguous patterns. *Current Biology, 13*(13), 1076–1085. doi:10.1016/S0960-9822(03)00414-7

Malach, R. (2012). Targeting the functional properties of cortical neurons using fMR-adaptation. *NeuroImage, 62*(2), 1163–1169. doi:10.1016/j.neuroimage.2012.01.002

Martinez-Trujillo, J. C., Tsotsos, J. K., Simine, E., Pomplun, M., Wildes, R., Treue, S., … Hopf, J.-M. (2005). Selectivity for speed gradients in human area MT/V5. *Neuroreport*, *16*(5), 435–438.

Morrone, M. C., Burr, D. C., & Vaina, L. M. (1995). Two stages of visual processing for radial and circular motion. *Nature, 376*(6540), 507–509. doi:10.1038/376507a0

Movshon, J. A., & Newsome, W. T. (1996). Visual response properties of striate cortical neurons projecting to area MT in macaque monkeys. *J Neurosci, 16*(23), 7733–7741.

Nawrot, M., & Blake, R. (1989). Neural integration of information specifying structure from stereopsis and motion. *Science (New York, N.Y.), 244*(4905), 716–718. doi:10.1126/science.2717948

Nawrot, M., & Blake, R. (1991). The interplay between stereopsis and structure from motion. *Perception & Psychophysics, 49*(3), 230–244. doi:10.3758/BF03214308

Noest, A. J., van Ee, R., Nijs, M. M., & van Wezel, R. J. A. (2007). Percept-choice sequences driven by interrupted ambiguous stimuli: A low-level neural model. *Journal of Vision, 7*(8), 10. doi:10.1167/7.8.10

Noest, A. J., & van Wezel, R. J. A. (2012). Dynamics of temporally interleaved percept-choice sequences: Interaction via adaptation in shared neural populations. *Journal of Computational Neuroscience, 32*(1), 177–195. doi:10.1007/s10827-011-0347-7

Orbach, J., Ehrlich, D., & Heath, H. A. (1963). Reversibility of the Necker cube. I. An examination of the concept of "satiation of orientation". *Perceptual and Motor Skills, 17,* 439–458. doi:10.2466/pms.1963.17.2.439

Orban, G. A. (2011). The extraction of 3D shape in the visual system of human and nonhuman primates. *Annual Review of Neuroscience, 34,* 361–388. doi:10.1146/annurev-neuro-061010-113819

Orban, G. A., Fize, D., Peuskens, H., Denys, K., Nelissen, K., Sunaert, S., … Vanduffel, W. (2003). Similarities and differences in motion processing between the human and macaque brain: Evidence from fMRI. *Neuropsychologia*, *41*(13), 1757–1768. doi:10.1016/S0028-3932(03)00177-5

Pastukhov, A., & Braun, J. (2008). A short-term memory of multi-stable perception. *Journal of Vision, 8*(13), 7.1–14. doi:10.1167/8.13.7

Pastukhov, A., & Braun, J. (2011). Cumulative history quantifies the role of neural adaptation in multistable perception. *Journal of Vision, 11*(10), 12. doi:10.1167/11.10.12

Pastukhov, A., & Braun, J. (2013a). Disparate time-courses of adaptation and facilitation in multi-stable perception. *Learning & Perception, 5*(s2), 101–118. doi:10.1556/LP.5.2013.Suppl2.7

Pastukhov, A., & Braun, J. (2013b). Structure-from-motion: Dissociating perception, neural persistence, and sensory memory of illusory depth and illusory rotation. *Attention, Perception & Psychophysics, 75*(2), 322–340. doi:10.3758/s13414-012-0390-0

Pastukhov, A., Füllekrug, J., & Braun, J. (2013). Sensory memory of structure-from-motion is shape-specific. *Attention, Perception & Psychophysics, 75*(6), 1215–1229. doi:10.3758/s13414-013-0471-8

Pearson, J., & Brascamp, J. W. (2008). Sensory memory for ambiguous vision. *Trends in Cognitive Sciences, 12*(9), 334–341. doi:10.1016/j.tics.2008.05.006

Petersik, T. J. (2002). Buildup and decay of a three-dimensional rotational aftereffect obtained with a three-dimensional figure. *Perception, 31*(7), 825–836. doi:10.1068/p3358

Peuskens, H., Claeys, K. G., Todd, J. T., Norman, J. F., Van Hecke, P., & Orban, G. A. (2004). Attention to 3-D shape, 3-D motion, and texture in 3-D structure from motion displays. *Journal of Cognitive Neuroscience, 16*(4), 665–682. doi:10.1162/089892904323057371

Preston, T. J., Kourtzi, Z., & Welchman, A. E. (2009). Adaptive estimation of three-dimensional structure in the human brain. *The Journal of Neuroscience: The Official Journal of the Society for Neuroscience, 29*(6), 1688–1698. doi:10.1523/JNEUROSCI.5021-08.2009

Raiguel, S., Van Hulle, M. M., Xiao, D. K., Marcar, V. L., Lagae, L., & Orban, G. A. (1997). Size and shape of receptive fields in the medial superior temporal area (MST) of the macaque. *Neuroreport, 8*(12), 2803–2808.

Ross, T. D. (2003). Accurate confidence intervals for binomial proportion and Poisson rate estimation. *Computers in Biology and Medicine, 33*(6), 509–531. doi:10.1016/S0010-4825(03)00019-2

Rust, N. C., Mante, V., Simoncelli, E. P., & Movshon, J. A. (2006). How MT cells analyze the motion of visual patterns. *Nature Neuroscience, 9*(11), 1421–1431. doi:10.1038/nn1786

Schacter, D. L., Wig, G. S., & Stevens, W. D. (2007). Reductions in cortical activity during priming. *Current Opinion in Neurobiology, 17*(2), 171–176. doi:10.1016/j.conb.2007.02.001

Schwiedrzik, C. M., Ruff, C. C., Lazar, A., Leitner, F. C., Singer, W., & Melloni, L. (2012). Untangling perceptual memory: Hysteresis and adaptation map into separate cortical networks. *Cerebral Cortex*. doi:10.1093/cercor/bhs396

Segaert, K., Weber, K., de Lange, F. P., Petersson, K. M., & Hagoort, P. (2013). The suppression of repetition enhancement: A review of fMRI studies. *Neuropsychologia, 51*(1), 59–66. doi:10.1016/j.neuropsychologia.2012.11.006

Shechter, S., Hochstein, S., & Hillman, P. (1988). Shape similarity and distance disparity as apparent motion correspondence

cues. *Vision Research, 28*(9), 1013–1021. doi:10.1016/0042-6989(88)90078-8

Sincich, L. C., & Horton, J. C. (2005). The circuitry of V1 and V2: Integration of color, form, and motion. *Annual Review of Neuroscience, 28,* 303–326. doi:10.1146/annurev.neuro.28.061604.135731

Smith, A. T., & Wall, M. B. (2008). Sensitivity of human visual cortical areas to the stereoscopic depth of a moving stimulus. *Journal of Vision, 8*(10), 1.1–12. doi:10.1167/8.10.1

Smith, A. T., Wall, M. B., Williams, A. L., & Singh, K. D. (2006). Sensitivity to optic flow in human cortical areas MT and MST. *The European Journal of Neuroscience, 23*(2), 561–569. doi:10.1111/j.1460-9568.2005.04526.x

Sperling, G., & Dosher, B. A. (1994). Depth from motion. In T. V. Papathomas, A. G. Charles Chubb, & E. Kowler (Eds.), *Early vision and beyond* (pp. 133–142). Cambridge, MA: MIT Press.

Sterzer, P., & Rees, G. (2008). A neural basis for percept stabilization in binocular rivalry. *Journal of Cognitive Neuroscience, 20*(3), 389–399. doi:10.1162/jocn.2008.20039

Tanaka, K., Fukada, Y., & Saito, H. A. (1989). Underlying mechanisms of the response specificity of expansion/contraction and rotation cells in the dorsal part of the medial superior temporal area of the macaque monkey. *Journal of Neurophysiology, 62*(3), 642–656.

Tanaka, Y., & Sagi, D. (1998). A perceptual memory for low-contrast visual signals. *Proceedings of the National Academy of Sciences of the United States of America, 95*(21), 12729–12733. doi:10.1073/pnas.95.21.12729

Van Essen, D. C., Maunsell, J. H., & Bixby, J. L. (1981). The middle temporal visual area in the macaque: Myeloarchitecture, connections, functional properties and topographic organization. *The Journal of Comparative Neurology, 199*(3), 293–326. doi:10.1002/cne.901990302

Wallach, H., & O'Connell, D. N. (1953). The kinetic depth effect. *Journal of Experimental Psychology, 45*(4), 205–217. doi:10.1037/h0056880

Walther, C., Schweinberger, S. R., Kaiser, D., & Kovács, G. (2012). Neural correlates of priming and adaptation in familiar face perception. *Cortex; A Journal Devoted to the Study of the Nervous System and Behavior*, 1–15. doi:10.1016/j.cortex.2012.08.012

Webster, M. A. (2011). Adaptation and visual coding. *Journal of Vision, 11*(5), 1–23. doi:10.1167/11.5.3

Wolfe, J. M. (1984). Reversing ocular dominance and suppression in a single flash. *Vision Research, 24*(5), 471–478. doi:10.1016/0042-6989(84)90044-0

Yu, K. (2000). Can semantic knowledge influence motion correspondence? *Perception, 29*(6), 693–707. doi:10.1068/p3063